АВТОМАТИЧЕСКОЕ УПРАВЛЕНИЕ И РОБОТОТЕХНИКА

AUTOMATIC CONTROL AND ROBOTICS

doi: 10.17586/2226-1494-2026-26-4-753-762

Saturation-enhanced dynamic regressor extension for robust carrier frequency estimation of disturbed amplitude-modulated signals

Duc Long Hoang[1]✉, Anton A. Pyrkin[2]

[1] Le Quy Don Technical University, Hanoi, 10065, Vietnam
[2] ITMO University, Saint Petersburg, 197101, Russian Federation

[1] longhd@lqdtu.edu.vn✉, https://orcid.org/0000-0003-4975-9547
[2] pyrkin@itmo.ru, https://orcid.org/0000-0001-8806-4057

Abstract
This paper considers the problem of carrier frequency estimation from measurements of an amplitude-modulated signal in the presence of unknown bounded disturbances and a time-varying envelope. Existing identification methods based on regression transformations usually require a small-disturbance condition, which limits their practical applicability. The scientific novelty of this work consists in the development of a robust carrier-frequency estimation algorithm that preserves the regression structure of delay-based signal parameterization and does not require the assumption of small disturbance magnitude. The proposed method is based on the parameterization of the measured signal using delayed measurements, which makes it possible to reduce the problem to a linear regression model. To estimate the unknown parameter, an adaptive algorithm with a saturation nonlinearity is used, limiting the influence of large regression errors. After estimating the regression parameter, the carrier frequency is reconstructed. The effectiveness of the proposed method is verified through numerical experiments for amplitude-modulated signals under noise and impulsive disturbances. A comparison with a normalized gradient algorithm and a power-transformed regression method is performed. The simulation results demonstrate a faster reduction of the estimation error and improved robustness of the proposed algorithm. The obtained results show the advantage of the proposed method over existing frequency-estimation algorithms under strong disturbances. The method can be applied to radio-signal processing, communication systems, and modulation-recognition algorithms. Future research directions include the development of discrete-time implementations of the algorithm and its extension to multi-component signals.

Keywords
amplitude-modulated signal, carrier frequency estimation, delay parameterization, nonlinear disturbance attenuation, dynamic regressor extension, robust adaptive identification, saturation nonlinearity, impulsive noise

Acknowledgements
The work was supported by the Russian Science Foundation (project No. 25-29-00896). The authors would like to thank the support of colleagues at the Department of Automation and Computing Techniques, Le Quy Don Technical University, Hanoi, Vietnam.

For citation: Hoang D.L., Pyrkin A.A. Saturation-enhanced dynamic regressor extension for robust carrier frequency estimation of disturbed amplitude-modulated signals. *Scientific and Technical Journal of Information Technologies, Mechanics and Optics*, 2026, vol. 26, no. 4, pp. 753–762. doi: 10.17586/2226-1494-2026-26-4-753-762

УДК 681.51.015

Расширение динамического регрессора с насыщением для робастной оценки частоты несущей возмущенных амплитудно-модулированных сигналов

Дык Лонг Хоанг[1]✉, Антон Александрович Пыркин[2]

[1] Технический Университет Ле Куй Дона, Ханой, 10065, Вьетнам
[2] Университет ИТМО, Санкт-Петербург, 197101, Российская Федерация

[1] longhd@lqdtu.edu.vn✉, https://orcid.org/0000-0003-4975-9547
[2] pyrkin@itmo.ru, https://orcid.org/0000-0001-8806-4057

Аннотация

Введение. Рассмотрена задача оценки частоты несущей по измерениям амплитудно-модулированного сигнала в присутствии неизвестных ограниченных возмущений и изменяющейся огибающей. Существующие методы идентификации, основанные на регрессионных преобразованиях, как правило, требуют выполнения условия малости возмущений, что ограничивает их практическое применение. Научная новизна работы заключается в разработке робастного алгоритма оценки частоты несущей, который сохраняет регрессионную структуру параметризации сигнала на основе задержки и не требует предположения о малой величине возмущений. **Метод.** Предложенный метод основан на параметризации измеренного сигнала с использованием задержанных измерений, что позволяет свести задачу к линейной регрессионной модели. Для оценки неизвестного параметра применен адаптивный алгоритм с нелинейностью насыщения, ограничивающей влияние больших ошибок регрессии. После оценки регрессионного параметра выполняется восстановление частоты несущей. **Основные результаты.** Эффективность представленного метода проверена в численных экспериментах для амплитудно-модулированных сигналов в условиях шумов и импульсных возмущений. Проведено сравнение с нормализованным градиентным алгоритмом и методом степенного преобразования регрессии. Результаты моделирования показали более быстрое уменьшение ошибки оценки и более высокую устойчивость предложенного алгоритма. **Обсуждение.** Полученные результаты демонстрируют преимущество разработанного метода по сравнению с существующими алгоритмами оценки частоты в условиях сильных возмущений. Метод может быть применен в задачах обработки радиосигналов, системах связи и алгоритмах распознавания модуляции. Перспективными направлениями дальнейших исследований являются разработка дискретных реализаций алгоритма и его расширение на случай многокомпонентных сигналов.

Ключевые слова

амплитудно-модулированный сигнал, оценка частоты несущей, параметризация с использованием задержек, нелинейное подавление возмущений, расширение динамического регрессора, робастная адаптивная идентификация, нелинейность насыщения, импульсный шум

Благодарности

Работа выполнена при финансовой поддержке Российского научного фонда (проект № 25-29-00896). Авторы выражают благодарность за поддержку коллегам кафедры автоматизации и вычислительной техники, Технический университет Ле Куй Дона, Ханой, Вьетнам.

Ссылка для цитирования: Хоанг Д.Л., Пыркин А.А. Расширение динамического регрессора с насыщением для робастной оценки частоты несущей возмущенных амплитудно-модулированных сигналов // Научно-технический вестник информационных технологий, механики и оптики. 2026. Т. 26, № 4. С. 753–762 (на англ. яз.). doi: 10.17586/2226-1494-2026-26-4-753-762

Introduction

Carrier frequency estimation remains a central task in sensing, communications, and control, especially when measurements contain colored noise, structured interference, or outliers, and when signal amplitudes vary over time. Recent work has continued advancing both spectral estimators (including refined interpolation and iterative equalization ideas) and model-based adaptive estimators that operate online and provide stability guarantees. For example, modern discrete-time Fourier techniques have been improved through interpolation strategies and efficient coarse-to-fine refinements [1–3], while notch-filter-based adaptive schemes remain attractive for real-time operation [4, 5]. In parallel, adaptive identification has benefited from the dynamic regressor extension and mixing methodology and its ongoing theoretical development, including relaxed convergence conditions and bias analyses under perturbations [6, 7]. Prescribed-time and finite-time estimation ideas also continue to grow for sinusoidal parameter identification in challenging environments [8, 9].

A particularly relevant recent contribution reformulates the disturbed amplitude-modulated carrier estimation problem into a linear regression by using delayed versions of the measured signal and then reduces disturbance impact through a power-type nonlinear transformation combined with dynamic regressor extension and mixing [10]. That approach yields a clear disturbance admissibility bound ensuring the transformed disturbance remains sufficiently small (in magnitude) for the subsequent identification stage. However, practical sensing chains often experience intermittent saturation, impulsive bursts, or interference levels that violate such smallness requirements.

The assumption that the modulation envelope is available is realistic in several engineering scenarios. For instance, during radio-frequency front-end calibration, carrier synchronization tests, or laboratory validation of communication receivers, the amplitude modulation law is generated by a signal generator or by a digital baseband unit and is therefore available as a commanded reference, whereas the actual carrier frequency may still be unknown due to oscillator drift, Doppler shift, or frequency mismatch between the transmitter and the receiver. A similar situation also appears when pilot or training signals with known amplitude envelopes are used for online carrier recovery. If the available envelope is measured or is nominal rather than exact, the resulting bounded envelope mismatch can be treated as an additional bounded disturbance, which is consistent with the robust formulation adopted in this paper. Our method is conceptually aligned with robust innovation limiting used across estimation and control [11, 12] and is complementary to learning-based modulation recognition pipelines that still require reliable front-end frequency estimates [13, 14]. We provide new lemmas and theorems establishing boundedness and explicit ultimate error bounds, and we validate the design via comparisons against more than two representative prior algorithms: the power-transformed regression identification scheme [10]; a classical normalized gradient identifier; a batch spectral interpolation estimator representative of modern frequency-domain practice [15].

Problem Formulation

We consider the measured signal [10]

$$y(t) = A_m(t)\sin(\omega t + \varphi) + \delta_{\text{eff}}(t), \quad t \geq 0, \tag{1}$$

where $y(t) \in \mathbb{R}$ is a measured signal; $A_m(t) > 0$ is the available commanded, calibrated, or independently measured amplitude envelope; $\omega > 0$ is an unknown constant carrier angular frequency; $\varphi \in \mathbb{R}$ is an unknown constant phase; $\delta_{\text{eff}}(t) \in \mathbb{R}$ is an unknown bounded effective disturbance. If the true envelope is $A(t) = A_m(t) + \varepsilon_A(t)$, then

$$y(t) = A(t)\sin(\omega t + \varphi) + \delta(t), \tag{2}$$

where $\varepsilon_A(t)$ is a bounded envelope mismatch and $\delta(t)$ is the original additive disturbance. The representation in (2) shows how the original additive disturbance and the envelope mismatch are incorporated into the measured signal model. The effective disturbance is then written as

$$\delta_{\text{eff}}(t) = \delta(t) + \varepsilon_A(t)\sin(\omega t + \varphi).$$

Hence, bounded envelope mismatch is absorbed into the effective disturbance term. The rigorous theoretical analysis below is established for a constant carrier frequency ω and a constant phase φ. When the carrier frequency or phase varies slowly, the proposed estimator may be interpreted as a robust online tracking algorithm; however, exact convergence guarantees for rapidly time-varying carrier dynamics are not claimed in this paper and are left for future work.

Since the available envelope satisfies $A_m(t) \geq A_{\min} > 0$, the measured signal may be normalized as

$$z_y(t) = \frac{y(t)}{A_m(t)}. \tag{3}$$

Then

$$z_y(t) = \sin(\omega t + \varphi) + \delta_z(t), \quad \delta_z(t) = \frac{\delta_{\text{eff}}(t)}{A_m(t)}.$$

Therefore,

$$|\delta_z(t)| \leq \frac{\bar{\delta}_{\text{eff}}}{A_{\min}}. \tag{4}$$

The normalization formulas (3) and (4) show that the preliminary division by $A_m(t)$ does not remove the disturbance, but only rescales its upper bound. Thus, normalization is a valid preprocessing step, but it does not remove the disturbance; it only rescales its effective bound.

Design an online estimator $\hat{\omega}(t)$ such that all internal signals of the estimation algorithm remain bounded for all $t \geq 0$, and the frequency estimation error

$$\tilde{\omega}(t) = \hat{\omega}(t) - \omega \tag{5}$$

is uniformly ultimately bounded, i.e., it converges to a computable neighborhood of zero under explicit assumptions. The estimation problem is therefore formulated in terms of the frequency error defined in (5).

Assumptions:

Assumption A1 (Available envelope and bounds). The amplitude envelope $A_m(t)$ used by the estimator is available as a commanded, calibrated, or independently measured signal. It is continuously differentiable and bounded as

$$0 < A_{\min} \leq A_m(t) \leq A_{\max} < \infty, \tag{6}$$

where $A_{\min}$ and $A_{\max}$ are known constants. The bounds in (6) guarantee that the available envelope is nonzero and that the normalization in (3) is well-defined.

Assumption A2 (Carrier range). The unknown ω lies in a known interval

$$\omega \in [\omega_{\min}, \omega_{\max}],\ 0 < \omega_{\min} < \omega_{\max}. \tag{7}$$

The carrier-frequency interval in (7) is used later to guarantee the uniqueness of the inverse mapping from the regression parameter to the frequency.

Assumption A3 (Bounded disturbance). The effective disturbance acting on the measured signal is bounded

$$|\delta_{\text{eff}}(t)| \leq \bar{\delta}_{\text{eff}}, \quad \forall t \geq 0, \tag{8}$$

where $\bar{\delta}_{\text{eff}}$ is known or conservatively upper-bounded. The term $\delta_{\text{eff}}(t)$ may include measurement noise, external interference, impulsive outliers with bounded amplitude, and bounded mismatch between the true amplitude envelope and the envelope available to the estimator. The disturbance bound in (8) is used in the Lyapunov analysis of Theorem 1.

Assumption A4 (Delay feasibility). A design delay $d_1 > 0$ is chosen such that

$$\sin(\omega d_1) \neq 0 \text{ for all } \omega \in [\omega_{\min}, \omega_{\max}], \tag{9}$$

which holds, for example, if $[\omega_{\min} d_1, \omega_{\max} d_1]$ avoids integer multiples of π. Condition (9) prevents singular delay choices and is used in Lemma 2.

Define delayed measurements for the constant delays d_1 and d_2 as

$$y_1(t) = y(t - d_1), \quad y_2(t) = y(t - d_2) \tag{10}$$

for $t \geq \max\{d_1, d_2\}$.

Choose $d_2 = 2d_1$. Following the delay-algebra strategy used in [10], one can construct signals $z(t)$ and $\varphi(t)$ such that the measured data satisfy a scalar linear regression

$$z(t) = \phi(t)\eta + \Delta(t), \tag{11}$$

where $\eta \triangleq 2\cos(\omega d_1)$ is an unknown constant parameter; $z(t)$ and $\phi(t)$ are known, computable signals constructed from $y(t)$, $y_1(t)$, $y_2(t)$, and the available envelope $A_m(t)$; $\Delta(t)$ is the induced regression disturbance which depends on the delayed effective disturbances and possible bounded envelope mismatch, but is unknown in value. Here and below, $\phi(t)$ denotes the known time-varying regression signal and should not be confused with φ in (1), which denotes the unknown constant phase of the carrier signal. These two symbols are intentionally kept different because they describe different quantities. The delayed measurements in (10) are used to construct the scalar regression model in (11).

Define the scalar saturation

$$\mathrm{sat}(x;\rho) = \begin{cases} \rho, & x > \rho \\ x, & |x| \le \rho \\ -\rho, & x < -\rho \end{cases}, \tag{12}$$

where $\rho > 0$ is a design constant.

Let the instantaneous regression residual be

$$e(t) = z(t) - \phi(t)\hat{\eta}(t), \tag{13}$$

where $\hat{\eta}(t)$ is an estimate of the parameter η.

We propose the saturation-normalized gradient update

$$\dot{\hat{\eta}}(t) = \gamma \frac{\phi(t)}{1 + \phi^2(t)} \mathrm{sat}(e(t);\rho), \tag{14}$$

where $\gamma > 0$ is an adaptation gain.

After estimating $\hat{\eta}(t)$, reconstruct $\tilde{\omega}(t)$ via

$$\hat{\omega}(t) = \frac{1}{d_1} \arccos\left(\frac{\prod(\hat{\eta}(t))}{2}\right), \tag{15}$$

where $\prod(\cdot)$ is a projection to enforce $\prod(\hat{\eta}) \in [-2, 2]$,

$$\prod(\hat{\eta}) = \min\{2\max\{-2, \hat{\eta}\}\}. \tag{16}$$

Equations (15) and (16) define the complete frequency-reconstruction stage from the estimated regression parameter.

Theoretical Analysis

To establish the basic well-posedness of the proposed adaptive law, we first show that the innovation-limited update remains uniformly bounded for all admissible values of the regression residual.

Lemma 1 (Boundedness of innovation-limited update).

For all $t \ge 0$,

$$|\dot{\hat{\eta}}(t)| \le \frac{\gamma\rho}{2}. \tag{17}$$

Proof.

By the definition (12), it has

$$|\mathrm{sat}(e(t);\rho)| \le \rho. \tag{18}$$

From the update law (14),

$$\left|\dot{\hat{\eta}}(t)\right| = \gamma \left|\frac{\phi(t)}{1 + \phi^2(t)}\right| |\mathrm{sat}(e(t);\rho)|. \tag{19}$$

Substituting (18) into (19) gives

$$\left|\dot{\hat{\eta}}(t)\right| \le \gamma\rho \left|\frac{\phi(t)}{1 + \phi^2(t)}\right|. \tag{20}$$

We now bound the scalar function $g(\phi) = \frac{|\phi|}{1 + \phi^2}$ for any $\phi \in \mathbb{R}$. It has $2|\phi| \le 1 + \phi^2$. Hence, for all $\phi \in \mathbb{R}$

$$\frac{|\phi|}{1 + \phi^2} \le \frac{1}{2}. \tag{21}$$

Combine (20) and (21)

$$\left|\dot{\hat{\eta}}(t)\right| \le \gamma\rho\frac{1}{2} = \frac{\gamma\rho}{2}. \tag{22}$$

Inequality (22) coincides with the required estimate in (17), which proves Lemma 1. ■

Next, in order to ensure that the unknown carrier frequency can be uniquely recovered from the identified constant parameter η, we analyze the parameterization in Lemma 2 below.

Lemma 2 (Local invertibility and uniqueness of ω from η over a known range).

Suppose Assumption A4 holds. Then the mapping

$$\eta(\omega) = 2\cos(\omega d_1) \tag{23}$$

is one-to-one over $\omega \in [\omega_{\min}, \omega_{\max}]$ if the interval length satisfies

$$\sin(\omega d_1) \ne 0 \text{ for all } \omega \in [\omega_{\min}, \omega_{\max}] \tag{24}$$

$$(\omega_{\max} - \omega_{\min})d_1 < \pi. \tag{25}$$

In that case, ω can be uniquely constructed from η within $[\omega_{\min}, \omega_{\max}]$.

Proof.

Since d_1 is constant, the derivative of (23) exists and equals

$$\frac{d\eta}{d\omega}(\omega) = -2d_1\sin(\omega d_1). \tag{26}$$

Combine (24) and (26), it has

$$\frac{d\eta}{d\omega}(\omega) \ne 0 \quad \forall\omega \in [\omega_{\min}, \omega_{\max}]. \tag{27}$$

Consider the image interval for the argument of sine:

$$\theta = \omega d_1 \in [\omega_{\min}d_1, \omega_{\max}d_1]. \tag{28}$$

The nonzero derivative condition in (27) and the interval representation in (28) are used to prove that the mapping $\omega \mapsto \eta$ is strictly monotone. By (25), so the interval $[\omega_{\min}d_1, \omega_{\max}d_1]$ has length strictly smaller than π. Now note that zeros of $\sin\theta$ occur at $\theta = k\pi$, $k \in \mathbb{Z}$. Because of (24), the interval $[\omega_{\min}d_1, \omega_{\max}d_1]$ contains no point $k\pi$. Together with the length condition (25), this implies the interval cannot cross from a region where $\sin\theta > 0$ to a region where $\sin\theta < 0$. Therefore, there exists a constant sign $s \in \{+1, -1\}$ such that

$$s \cdot \sin(\omega d_1) > 0 \quad \forall\omega \in [\omega_{\min}, \omega_{\max}]. \tag{29}$$

Substituting (29) into the derivative formula (26) shows that $\frac{d\eta}{d\omega}(\omega)$ has a constant nonzero sign on $[\omega_{\min}, \omega_{\max}]$. Hence $\eta(\omega)$ is strictly monotone on the interval

$$\omega_1 < \omega_2 \Rightarrow \eta(\omega_1) \neq \eta(\omega_2), \quad \forall \omega_1, \omega_2 \in [\omega_{\min}, \omega_{\max}]. \tag{30}$$

Assume, for contradiction, that there exist $\omega_1 \neq \omega_2$ in $[\omega_{\min}, \omega_{\max}]$ such that

$$\eta(\omega_1) = \eta(\omega_2). \tag{31}$$

Without loss of generality, let $\omega_1 < \omega_2$. But strict monotonicity (30) implies $\eta(\omega_1) \neq \eta(\omega_2)$, contradicting (31). Thus, no such pair can exist, i.e., the map $\omega \mapsto \eta$ is one-to-one on $[\omega_{\min}, \omega_{\max}]$. Therefore, for each η generated by (23) with $\omega \in [\omega_{\min}, \omega_{\max}]$, there is exactly one $\omega \in [\omega_{\min}, \omega_{\max}]$ satisfying (23).

The following theorem proves global boundedness of the estimation process and derives an explicit ultimate bound for the parameter estimation error $\tilde{\eta}(t)$ under bounded disturbance and persistent excitation conditions.

Theorem 1 (Global boundedness and ultimate bound for $\tilde{\eta}$).

Assume the regression (11) holds with bounded disturbance $|\Delta(t)| \leq \Delta_{\max}$. Consider the proposed update law with constants $\gamma > 0$ and $\rho > 0$. Then

1. $\hat{\eta}(t)$ is globally bounded for all initial conditions;

2. the estimation error $\tilde{\eta}(t) = \hat{\eta}(t) - \eta$ is uniformly ultimately bounded, with an ultimate bound proportional to $\min\{\Delta_{\max}, \rho\}$. In particular, if $\phi(t)$ is persistently exciting in the standard scalar sense, there exist constants $T > 0$ and $\mu > 0$ such that

$$\int_t^{t+T} \frac{\phi^2(t)}{1+\phi^2(t)} d\tau \geq \mu, \quad \forall t \geq 0. \tag{32}$$

Here, τ is the dummy variable of integration, and $\phi^2(\tau)$ denotes $(\phi(\tau))^2$, where $\phi(\tau)$ is the known scalar regression signal defined in (11). Then $\tilde{\eta}(t)$ is uniformly ultimately bounded, and one can bound the ultimate error by an explicit constant proportional to $\min\{\Delta_{\max}, \rho\}$:

$$\limsup_{t\to\infty} \left|\tilde{\eta}(t)\right| \leq \frac{T}{2\mu} \min\{\Delta_{\max}, \rho\}. \tag{33}$$

Proof.

From (11) and the definition of $e(t)$ in (13)

$$e(t) = -\phi(t)\tilde{\eta}(t) + \Delta(t). \tag{34}$$

Also, since η is constant, $\dot{\tilde{\eta}}(t) = \dot{\hat{\eta}}(t)$. Using (14)

$$\dot{\tilde{\eta}}(t) = \gamma \frac{\phi(t)}{1+\phi^2(t)} \mathrm{sat}(e(t); \rho). \tag{35}$$

Define the Lyapunov function

$$V(t) = \frac{1}{2}\tilde{\eta}^2(t). \tag{36}$$

Differentiating the Lyapunov function defined in (36) and using (35), we obtain

$$\dot{V}(t) = \tilde{\eta}(t)\dot{\tilde{\eta}}(t) = \gamma \frac{1}{1+\phi^2(t)} \phi(t)\tilde{\eta}(t)\mathrm{sat}(e(t); \rho). \tag{37}$$

The saturation $\mathrm{sat}(\cdot; \rho)$ is an odd, nondecreasing function with slope in [0, 1]. It satisfies the inequality

$$e(t)\,\mathrm{sat}(e(t); \rho) \geq (\mathrm{sat}(e(t); \rho))^2, \quad \forall t \geq 0. \tag{38}$$

From (34), it has

$$\phi(t)\tilde{\eta}(t) = \Delta(t) - e(t). \tag{39}$$

Substitute (39) into (37):

$$\dot{V}(t) = \gamma \frac{1}{1+\phi^2(t)} (\Delta(t) - e(t))\mathrm{sat}(e(t); \rho) = \\ = \gamma \frac{\Delta(t)\mathrm{sat}(e(t); \rho)}{1+\phi^2(t)} - \gamma \frac{e(t)\mathrm{sat}(e(t); \rho)}{1+\phi^2(t)}. \tag{40}$$

Now apply (38) to the second term

$$-\gamma \frac{e(t)\mathrm{sat}(e(t); \rho)}{1+\phi^2(t)} \leq -\gamma \frac{(\mathrm{sat}(e(t); \rho))^2}{1+\phi^2(t)}. \tag{41}$$

Thus

$$\dot{V}(t) \leq \gamma \frac{\Delta(t)\mathrm{sat}(e(t); \rho)}{1+\phi^2(t)} - \gamma \frac{(\mathrm{sat}(e(t); \rho))^2}{1+\phi^2(t)}. \tag{42}$$

From $|\Delta(t)| \leq \Delta_{\max}$ and $|\mathrm{sat}(e(t); \rho)| \leq \rho$ with $\forall t \geq 0$,

$$|\Delta(t)\mathrm{sat}(e(t); \rho)| \leq \Delta_{\max}\rho. \tag{43}$$

Therefore,

$$\dot{V}(t) \leq \gamma \frac{\Delta_{\max}\rho}{1+\phi^2(t)} - \gamma \frac{(\mathrm{sat}(e(t); \rho))^2}{1+\phi^2(t)}. \tag{44}$$

Inequalities (40)–(44) provide the basic dissipative estimate for the Lyapunov derivative in the presence of bounded regression disturbance. In particular, since $\frac{1}{1+\phi^2(t)} \leq 1$,

$$\dot{V}(t) \leq \gamma\Delta_{\max}\rho. \tag{45}$$

Inequality (45) shows that the Lyapunov function is locally absolutely continuous and that the estimator has no finite escape time under bounded $\Delta(t)$ and bounded $\mathrm{sat}(e(t); \rho)$. The uniform ultimate boundedness is then obtained below under the persistent excitation condition.

Let

$$c(t) \triangleq \frac{\phi^2(t)}{1+\phi^2(t)} \in [0, 1). \tag{46}$$

From (35) and (39),

$$\dot{\tilde{\eta}}(t) = -\gamma c(t)\tilde{\eta}(t) + \gamma \frac{\phi(t)}{1+\phi^2(t)} \Delta(t). \tag{47}$$

Using and $\left|\frac{\phi}{1+\phi^2}\right| \leq \frac{1}{2}$ and $|\Delta(t)| \leq \Delta_{\max}$, it obtains

$$\left|\gamma\frac{\phi(t)}{1+\phi^2(t)}\Delta(t)\right| \le \frac{\gamma}{2}\Delta_{\max}. \tag{48}$$

Moreover, since the limiter enforces $|\mathrm{sat}(e(t);\rho)| \le \rho$, the effective "input" cannot exceed ρ. This means the driving term is effectively bounded by $\min\{\Delta_{\max}, \rho\}$, and we define

$$\Delta_\rho \triangleq \min\{\Delta_{\max}, \rho\}. \tag{49}$$

The auxiliary definitions and estimates in (46)–(49) allow the error dynamics to be written in the scalar comparison form used below. Therefore, in the regime consistent with $|e(t)| \le \rho \Rightarrow |\mathrm{sat}(e(t);\rho)| \le \rho$, we can write the differential inequality

$$\frac{d}{dt}|\tilde\eta(t)| \le -\gamma c(t)|\tilde\eta(t)| + \frac{\gamma}{2}\Delta_\rho. \tag{50}$$

Now integrate (50) over any interval $[t, t+T]$. Using Grönwall-type arguments for scalar linear time-varying systems, one obtains the standard bound

$$|\tilde\eta(t+T)| \le e^{-\gamma\int_t^{t+T}c(\tau)d\tau}|\tilde\eta(t)| + \frac{\gamma}{2}\Delta_\rho\int_t^{t+T}e^{-\gamma\int_s^{t+T}c(\tau)d\tau}ds. \tag{51}$$

By the persistent excitation condition (32), for all $t \ge 0$,

$$\int_t^{t+T}c(\tau)d\tau \ge \mu. \tag{52}$$

Hence $e^{-\gamma\int_t^{t+T}c(\tau)d\tau} \le e^{-\gamma\mu}$, and also

$$\int_t^{t+T}e^{-\gamma\int_s^{t+T}c(\tau)d\tau}ds \le \int_t^{t+T}1ds = T. \tag{53}$$

Substitute (52) and (53) into (51):

$$|\tilde\eta(t+T)| \le e^{-\gamma\mu}|\tilde\eta(t)| + \frac{\gamma}{2}\Delta_\rho T. \tag{54}$$

Iterating (54) over successive intervals of length T yields a standard linear recursion, implying

$$\limsup_{t\to\infty}|\tilde\eta(t)| \le \frac{\frac{\gamma}{2}\Delta_\rho T}{1-e^{-\gamma\mu}}. \tag{55}$$

Using the inequality $1 - e^{-\gamma\mu} \ge \dfrac{\gamma\mu}{1+\gamma\mu}$, we obtain the simpler bound

$$\limsup_{t\to\infty}|\tilde\eta(t)| \le \frac{T}{2\mu}\Delta_\rho = \frac{(1+\gamma\mu)T}{2\mu}\min\{\Delta_{\max}, \rho\}. \tag{56}$$

The estimates (55) and (56) prove the ultimate bound stated in (33). The ultimate bound in (33) is later used to derive the practical stability of the reconstructed frequency estimate.

The following theorem shows that the reconstructed frequency estimate $\hat\omega(t)$ is practically stable and inherits the bounded-convergence property of $\hat\eta(t)$.

Theorem 2 (Practical stability of frequency estimate $\hat\omega$).

Under Assumptions A1-A4 and the conditions of Theorem 1, the frequency estimation error $\tilde\omega(t) = \hat\omega(t) - \omega$ is uniformly ultimately bounded. Moreover, if Lemma 2 uniqueness conditions hold, then there exists $c_\omega > 0$ such that

$$\limsup_{t\to\infty}|\tilde\omega(t)| \le c_\omega \limsup_{t\to\infty}|\tilde\eta(t)|. \tag{57}$$

Proof.

From (23), ω can be reconstructed from η by applying the inverse cosine on the correct branch. To guarantee that the argument of arccos(·) stays admissible, introduce the standard projection onto the feasible set [–2, 2]:

$$\Pi(\xi) = \begin{cases} 2, & \xi > 2, \\ \xi, & |\xi| \le 2, \\ -2, & \xi > -2, \end{cases} \tag{58}$$

and define the frequency estimate

$$\hat\omega(t) = \frac{1}{d_1}\arccos\left(\frac{\Pi(\hat\eta(t))}{2}\right), \tag{59}$$

where the branch of arccos(·) is selected as the unique one consistent with the known interval $[\omega_{\min}, \omega_{\max}]$.

Also define the true relation

$$\omega = \frac{1}{d_1}\arccos\left(\frac{\eta}{2}\right) \tag{60}$$

again with the same branch implied by $\omega \in [\omega_{\min}, \omega_{\max}]$.

Define the scalar function

$$F(\xi) = \frac{1}{d_1}\arccos\left(\frac{\xi}{2}\right). \tag{61}$$

Therefore,

$$|\tilde\omega(t)| = |\hat\omega(t) - \omega| = |F(\Pi(\hat\eta(t))) - F(\eta)|. \tag{62}$$

The reconstruction formula (59), the true relation (60), and the scalar function (61) are used to rewrite the frequency estimation error in (62). Hence it is sufficient to upper-bound (62) by multiplying $|\Pi(\tilde\eta(t)) - \eta|$ by a positive constant, and then relate $|\Pi(\hat\eta(t)) - \eta|$ to $|\hat\eta(t)) - \eta| = |\tilde\eta(t)|$.

Differentiate $F(\xi)$ for $\xi \in (-2, 2)$,

$$\frac{dF}{d\xi}(\xi) = \frac{1}{d_1}\frac{d}{d\xi}\arccos\left(\frac{\xi}{2}\right) = \frac{1}{d_1}\left(-\frac{1}{\sqrt{1-\left(\frac{\xi}{2}\right)^2}}\right)\frac{1}{2} = -\frac{1}{2d_1\sqrt{1-\left(\frac{\xi}{2}\right)^2}}. \tag{63}$$

If $\xi = \eta = 2\cos(\omega d_1)$, then

$$1-\left(\frac{\eta}{2}\right)^2 = 1-\cos^2(\omega d_1) = \sin^2(\omega d_1). \tag{64}$$

Thus, for values corresponding to $\omega \in [\omega_{\min}, \omega_{\max}]$,

$$\sqrt{1-\left(\frac{\eta}{2}\right)^2} = |\sin(\omega d_1)|. \tag{65}$$

By Lemma 2 condition, the continuous function $|\sin(\omega d_1)|$ attains a strictly positive minimum on the compact interval $[\omega_{min}, \omega_{max}]$. Define

$$s_{min} \triangleq \min_{\omega \in [\omega_{min}, \omega_{max}]} |\sin(\omega d_1)| > 0. \quad (66)$$

Consequently, for all ξ that belong to the image set $\{\eta(\omega) = 2\cos(\omega d_1): \omega \in [\omega_{min}, \omega_{max}]\}$, it has

$$\left|\frac{dF}{d\xi}(\xi)\right| \le \frac{1}{2d_1 s_{min}}. \quad (67)$$

Relations (63)–(66) provide a uniform bound for the derivative of $F(\xi)$, which is used in (67). Consider the two arguments in (62): $\xi_1 = \Pi(\hat{\eta}(t))$ and $\xi_2 = \eta$. The both lie in $[-2, 2]$ by construction and because $\eta = 2\cos(\omega d_1) \in [-2, 2]$. Because the correct branch of $\arccos(\cdot)$ is fixed by Lemma 2, F is single-valued and differentiable on the relevant subset. By the mean value theorem, there exists $\xi^*(t)$ between ξ_1 and ξ_2 such that

$$|F(\xi_1) - F(\xi_2)| = \left|\frac{dF}{d\xi}(\xi^*(t))\right| |\xi_1 - \xi_2|. \quad (68)$$

Using (67) in (68) gives

$$|\tilde{\omega}(t)| \le \frac{1}{2d_1 s_{min}} |\Pi(\hat{\eta}(t)) - \eta|. \quad (69)$$

The projection $\Pi(\cdot)$ in (58) is nonexpansive (1-Lipschitz) on $\mathbb{R}$

$$|\Pi(a) - \Pi(b)| \le |a - b|, \quad \forall a, b \in \mathbb{R}. \quad (70)$$

Since $\eta \in [-2, 2]$, it follows that $\Pi(\eta) = \eta$, hence from (70),

$$|\Pi(\hat{\eta}(t)) - \eta| = |\Pi(\hat{\eta}(t)) - \Pi(\eta)| \le |\hat{\eta}(t)) - \eta| = |\tilde{\eta}(t)|. \quad (71)$$

Substitute (71) into (69):

$$|\tilde{\omega}(t)| \le \frac{1}{2d_1 s_{min}} |\tilde{\eta}(t)| = c_\omega |\tilde{\eta}(t)|. \quad (72)$$

From Theorem 1, $\hat{\eta}(t)$ is uniformly ultimately bounded under the excitation condition. Taking $\limsup_{t\to\infty}$ on both sides of (72) yields

$$\limsup_{t\to\infty} |\tilde{\omega}(t)| \le c_\omega \limsup_{t\to\infty} |\tilde{\eta}(t)|. \quad (73)$$

Inequality (73) proves the practical frequency-error bound stated in (57). ■

Remark. In this paper, stability of the estimator is understood in the practical Lyapunov sense: all estimation signals are bounded, while the parameter and frequency estimation errors are uniformly ultimately bounded in the presence of bounded disturbances. Therefore, due to the nonzero disturbance term, exact asymptotic convergence to zero is not claimed in the general case; instead, convergence to an explicitly characterized neighborhood of zero is guaranteed.

Discussion

To evaluate the effectiveness of the proposed saturation-enhanced regression estimator, numerical simulations were conducted under conditions representative of disturbed amplitude-modulated measurements. The simulated signal follows the model defined in (1), where the carrier frequency is constant while the signal envelope varies slowly in time. Specifically, the true carrier frequency is set to $f_0 = 50$ Hz ($\omega = 2\pi f_0$) and the modulation envelope is chosen as $A(t) = 1 + 0.2\sin(2\pi\cdot 0.8t)$. The delay parameters used to construct the regression model (11) are $d_1 = 5$ ms, $d_2 = 10$ ms. For the proposed adaptive estimator (14), the design parameters are selected as $\gamma = 0.05$, $\rho = 0.5$. Three estimation algorithms are compared (using the same simulated signal and identical initial conditions): Proposed method; Normalized gradient estimator; Power-transformed regression estimator.

It should be noted that, when $A_m(t)$ is accurately available and satisfies $A_m(t) \ge A_{min} > 0$, the measurement may be preliminarily normalized by $A_m(t)$. This reduces the nominal carrier model to the unit-amplitude case. Nevertheless, the disturbance is transformed into $\frac{\delta_{eff}(t)}{A_m(t)}$, whose bound depends on A_{min}. Hence, normalization does not remove the disturbance; it only changes its effective bound. The proposed saturation-enhanced update remains applicable to both the original and normalized formulations.

In Fig. 1, the proposed saturation-enhanced estimator exhibits the fastest convergence, driving the error rapidly to zero within approximately 0.3 s. The normalized gradient method converges more slowly, while the power-transformed regression estimator shows a significantly longer transient period due to the nonlinear disturbance attenuation stage. These results confirm the improved convergence properties predicted by Theorem 1. In Fig. 2, the proposed method rapidly reconstructs the correct carrier frequency with minimal transient error and negligible steady-state deviation. The normalized gradient estimator also converges to the true frequency but with a longer settling time. The power-transformed regression estimator exhibits noticeably slower convergence, illustrating the

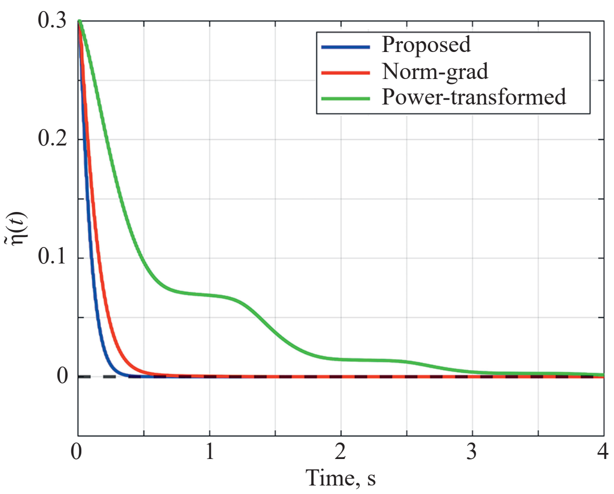

Fig. 1. Parameter estimation error $\tilde{\eta}(t) = \hat{\eta}(t) - \eta$

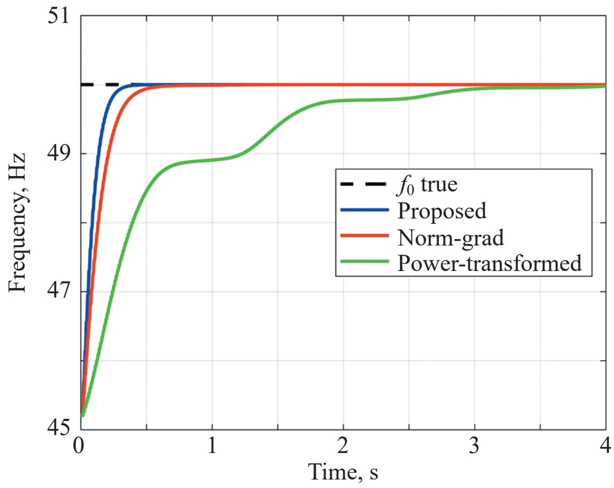

Fig. 2. Carrier frequency estimates $\hat{f} = \dfrac{\hat{\omega}(t)}{2\pi}$

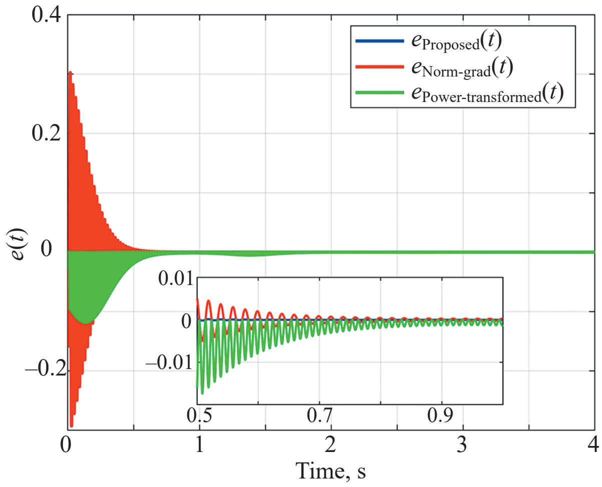

Fig. 3. Instantaneous regression residual $e(t)$

trade-off introduced by the disturbance transformation stage. In Fig. 3, the residual represents the mismatch between the measured signal and the regression model used for parameter identification. The proposed estimator suppresses the residual rapidly, demonstrating effective disturbance attenuation and fast parameter adaptation. The inset shows a magnified view of the early transient phase, highlighting the faster decay of the residual for the proposed method compared with the normalized gradient and power-transformed approaches.

To further evaluate the robustness of the proposed method under more realistic conditions, an additional simulation scenario was considered. In this test, the measured signal was affected by bounded envelope mismatch, slow carrier-frequency drift, bounded phase perturbation, random noise, high-frequency interference, and impulsive outliers:

$$y(t) = (A_m(t) + \varepsilon_A(t))\sin\left(\int_0^t \omega(\tau)d\tau + \varphi + \varepsilon_\varphi(t)\right) + \delta(t). \quad (74)$$

Equation (74) specifies the realistic test signal used for Fig. 4, where $A_m(t) = 1 + 0.2\sin(2\pi\cdot 0.8t)$ is the available envelope; $\varepsilon_A(t)$ is a bounded envelope mismatch; $\omega(t) = \omega_0 + 2\pi\varepsilon_f(t)$ is a slowly varying carrier angular frequency; $\varepsilon_\varphi(t)$ is a bounded phase perturbation. This test does not change the formal theoretical assumptions which are established for a constant carrier frequency, but

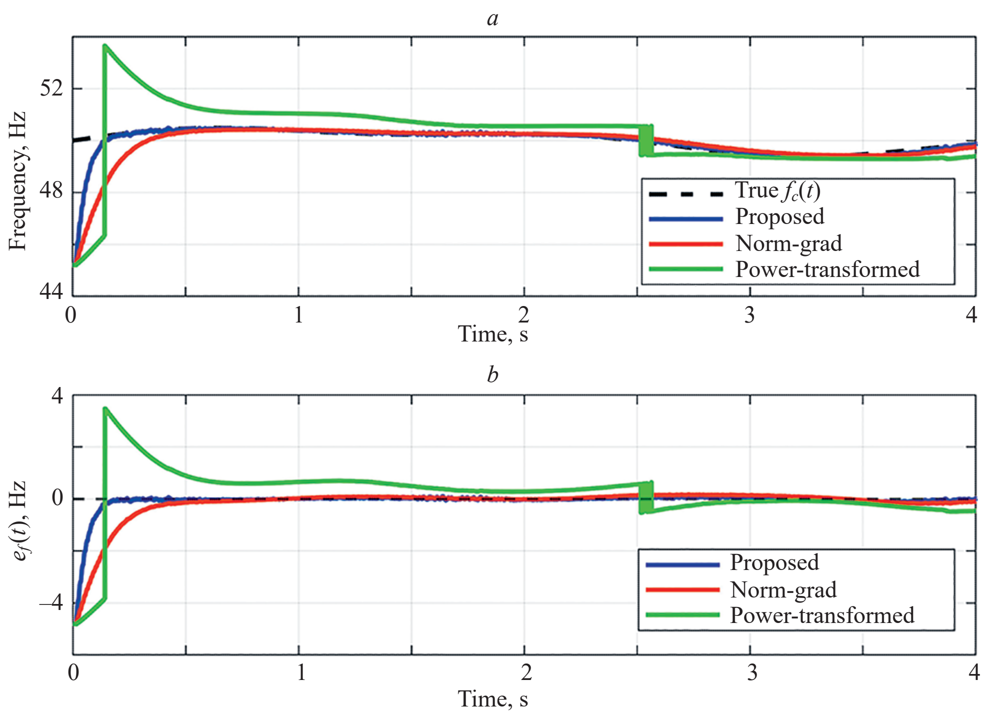

Fig. 4. Realistic scenario with bounded envelope mismatch, slow carrier-frequency drift, bounded phase perturbation, additive noise, high-frequency interference, and impulsive outliers: carrier frequency estimates (*a*); frequency tracking errors (*b*)

Table. Quantitative comparison under the realistic scenario with bounded envelope mismatch, slow carrier-frequency drift, bounded phase perturbation, and additive disturbances

Algorithm	$\hat{f}_{\text{final}}$, Hz	RMSE	MAE	Settling time, s
Proposed	49.87174704	0.379713692	0.095564724	0.3685
Norm-gradient	49.77326473	0.649615688	0.228681698	0.6620
Power-transformed	49.40465485	1.081341676	0.656847455	2.7375

it demonstrates the practical robustness of the estimator when bounded nonidealities are present.

Root Mean Square Error (RMSE) and Mean Absolute Error (MAE) indices are defined as

$$RMSE = \sqrt{\frac{1}{N_e}\sum_{k=k_0}^{N}(e_f(k))^2}, \quad (75)$$

$$MAE = \frac{1}{N_e}\sum_{k=k_0}^{N}|e_f(k)|, \quad (76)$$

where $e_f(k) = \hat{f}(k) - f_{\text{true}}(k)$, k_0 is the first valid estimation index after the delay interval; $N_e = N - k_0 + 1$ is the number of samples used for evaluation. The performance indices in (75) and (76) are used to compute the quantitative comparison reported in Table.

As shown in Fig. 4 and Table, the proposed saturation-enhanced estimator tracks the slowly varying carrier frequency more accurately than the normalized gradient and power-transformed regression estimators. The proposed method reaches the ±0.25 Hz error band after approximately 0.3685 s, while the normalized gradient estimator requires approximately 0.6620 s and the power-transformed estimator requires approximately 2.7375 s. These results support the claim that the proposed saturation-based adaptation improves robustness under realistic bounded imperfections. This additional test is used only as a robustness illustration. The formal convergence proof remains established for constant ω and constant φ.

Conclusion

This paper proposed a saturation-enhanced adaptive estimator for carrier frequency identification in disturbed amplitude-modulated signals. By combining delay-based regression modeling with an innovation-limited update law, the proposed method eliminates the need for the small-disturbance assumption commonly required in regression-based identification approaches. Theoretical analysis established boundedness of the estimator trajectories and provided an explicit ultimate bound for the parameter estimation error under bounded disturbances and persistent excitation. Simulation results demonstrated that the proposed algorithm achieves faster convergence and higher accuracy than both the classical normalized gradient estimator and the power-transformed regression approach. These results demonstrate the effectiveness of saturation-based disturbance attenuation for robust online frequency estimation. Future work will consider discrete-time implementations and extensions to multi-tone and time-varying frequency signals.

References

1. Russell F.P., Wilkinson K.A., Kelly P.H.J., Skylaris C.-K. Optimised three-dimensional Fourier interpolation: An analysis of techniques and application to a linear-scaling density functional theory code. *Computer Physics Communications*, 2015, vol. 187, pp. 8–19. doi: 10.1016/j.cpc.2014.09.019
2. Song H., Fan L., Liu J., Wu H., Li M., Qi G. Efficient frequency estimation of sinusoid based on autocorrelation and discrete time Fourier transform. *Circuits, Systems, and Signal Processing*, 2024, vol. 43, no. 7, pp. 4675–4689. doi: 10.1007/s00034-024-02670-w
3. Janeiro F.M., Ramos P M. Generalized Fractional Interpolated Discrete Fourier Transform with rectangular window for frequency estimation in noisy sinewave signals. *Metrology*, 2026, vol. 6, no. 1, pp. 8. doi: 10.3390/metrology6010008
4. Hinamoto Y., Doi A., Nishimura S. Adaptive normal state-space notch digital filters using gradient-descent method. *Circuits, Systems, and Signal Processing*, 2023, vol. 42, no. 7, pp. 3983–4001. doi: 10.1007/s00034-023-02297-3
5. M'Sirdi N.K., Monneau A., Naamane A. Adaptive notch filters for prediction of narrow band signals. *Proc. of the 7th International Conference on Systems and Control (ICSC)*, 2018, pp. 403–408. doi: 10.1109/ICoSC.2018.8587833
6. Ortega R., Aranovskiy S., Pyrkin A.A., Astolfi A., Bobtsov A.A. New results on parameter estimation via dynamic regressor extension and mixing: continuous and discrete-time cases. *IEEE Transactions on Automatic Control*, 2021, vol. 66, no. 5, pp. 2265–2272. doi: 10.1109/TAC.2020.3003651

Литература

1. Russell F.P., Wilkinson K.A., Kelly P.H.J., Skylaris C.-K. Optimised three-dimensional Fourier interpolation: An analysis of techniques and application to a linear-scaling density functional theory code // Computer Physics Communications. 2015. V. 187. P. 8–19. doi: 10.1016/j.cpc.2014.09.019
2. Song H., Fan L., Liu J., Wu H., Li M., Qi G. Efficient frequency estimation of sinusoid based on autocorrelation and discrete time Fourier transform // Circuits, Systems, and Signal Processing. 2024. V. 43. N 7. P. 4675–4689. doi: 10.1007/s00034-024-02670-w
3. Janeiro F.M., Ramos P M. Generalized Fractional Interpolated Discrete Fourier Transform with rectangular window for frequency estimation in noisy sinewave signals // Metrology. 2026. V. 6. N 1. P. 8. doi: 10.3390/metrology6010008
4. Hinamoto Y., Doi A., Nishimura S. Adaptive normal state-space notch digital filters using gradient-descent method // Circuits, Systems, and Signal Processing. 2023. V. 42. N 7. P. 3983–4001. doi: 10.1007/s00034-023-02297-3
5. M'Sirdi N.K., Monneau A., Naamane A. Adaptive notch filters for prediction of narrow band signals // Proc. of the 7th International Conference on Systems and Control (ICSC). 2018. P. 403–408. doi: 10.1109/ICoSC.2018.8587833
6. Ortega R., Aranovskiy S., Pyrkin A.A., Astolfi A., Bobtsov A.A. New results on parameter estimation via dynamic regressor extension and mixing: continuous and discrete-time cases // IEEE Transactions on Automatic Control. 2021. V. 66. N 5. P. 2265–2272. doi: 10.1109/TAC.2020.3003651

7. Taslima E., Kamal S., Saket R.K. Adaptive observer-based state and parameter estimation for two-level quantum systems using dynamic regressor extension and mixing. *Proc. of the 11th Indian Control Conference (ICC)*, 2025, pp. 247–252. doi: 10.1109/ICC69100.2025.11372417
8. Hu Y., Cheng C., Cai X., Peng J., Shi S. Prescribed-time sinusoidal signal parameter estimation: continuous-time design with discrete-time implementation for embedded systems. *Nonlinear Dynamics*, 2025, vol. 113, no. 18, pp. 24663–24675. doi: 10.1007/s11071-025-11425-4
9. Vediakova A.O., Vedyakov A.A., Pyrkin A.A., Bobtsov A.A., Gromov V.S. Finite time frequency estimation for multi-sinusoidal signals. *European Journal of Control*, 2021, vol. 59, pp. 38–46. doi: 10.1016/j.ejcon.2021.01.004
10. Bobtsov A.A., Oskina O.V., Slita O.V., Nikolaev N.A., Boitsev A.A. Harmonic carrier frequency estimation of a disturbed amplitude modulated signal. *Scientific and Technical Journal of Information Technologies, Mechanics and Optics*, 2026, vol. 26, no. 1, pp. 214–217. (in Russian). doi: 10.17586/2226-1494-2026-26-1-214-217
11. Chen K.-Y. A Real-time parameter estimation method by using disturbance observer-based control. *Journal of Dynamic Systems, Measurement, and Control*, 2020, vol. 142, no. 5, pp. 051005. doi: 10.1115/1.4046153
12. Chen R.-Z., Guo X.-G., Li Q., Wang J.-L., Guo L. Disturbance-observer-based model-free adaptive active fault-tolerant consensus control for MASs with TVDAF. *Automatica*, 2025, vol. 173, pp. 112114. doi: 10.1016/j.automatica.2025.112114
13. Han H., Yi Z., Zhu Z., Li L., Gong S., Li B., Wang M. Automatic modulation recognition based on deep-learning features fusion of signal and constellation diagram. *Electronics*, 2023, vol. 12, no. 3, pp. 552. doi: 10.3390/electronics12030552
14. Wang S., Yang K., Ji Z., Zhang Q., Pan H. Parameter estimation based automatic modulation recognition for radio frequency signal. *Proc. of the IEEE International Conference on Industry 4.0, Artificial Intelligence, and Communications Technology (IAICT)*, 2025, pp. 508–513. doi: 10.1109/IAICT65714.2025.11101466
15. Fan L., Qi G. Frequency estimator of sinusoid based on interpolation of three DFT spectral lines. *Signal Processing*, 2018, vol. 144, pp. 52–60. doi: 10.1016/j.sigpro.2017.09.028

7. Taslima E., Kamal S., Saket R.K. Adaptive observer-based state and parameter estimation for two-level quantum systems using dynamic regressor extension and mixing // Proc. of the 11th Indian Control Conference (ICC). 2025. P. 247–252. doi: 10.1109/ICC69100.2025.11372417
8. Hu Y., Cheng C., Cai X., Peng J., Shi S. Prescribed-time sinusoidal signal parameter estimation: continuous-time design with discrete-time implementation for embedded systems // Nonlinear Dynamics. 2025. V. 113. N 18. P. 24663–24675. doi: 10.1007/s11071-025-11425-4
9. Vediakova A.O., Vedyakov A.A., Pyrkin A.A., Bobtsov A.A., Gromov V.S. Finite time frequency estimation for multi-sinusoidal signals // European Journal of Control. 2021. V. 59. P. 38–46. doi: 10.1016/j.ejcon.2021.01.004
10. Бобцов А.А., Оськина О.В., Слита О.В., Николаев Н.А., Бойцев А.А. Оценка частоты гармонической несущей возмущенного амплитудно-модулированного сигнала // Научно-технический вестник информационных технологий, механики и оптики. 2026. Т. 26. № 1. С. 214–217. doi: 10.17586/2226-1494-2026-26-1-214-217
11. Chen K.-Y. A Real-time parameter estimation method by using disturbance observer-based control // Journal of Dynamic Systems, Measurement, and Control. 2020. V. 142. N 5. P. 051005. doi: 10.1115/1.4046153
12. Chen R.-Z., Guo X.-G., Li Q., Wang J.-L., Guo L. Disturbance-observer-based model-free adaptive active fault-tolerant consensus control for MASs with TVDAF // Automatica. 2025. V. 173. P. 112114. doi: 10.1016/j.automatica.2025.112114
13. Han H., Yi Z., Zhu Z., Li L., Gong S., Li B., Wang M. Automatic modulation recognition based on deep-learning features fusion of signal and constellation diagram // Electronics. 2023. V. 12. N 3. P. 552. doi: 10.3390/electronics12030552
14. Wang S., Yang K., Ji Z., Zhang Q., Pan H. Parameter estimation based automatic modulation recognition for radio frequency signal // Proc. of the IEEE International Conference on Industry 4.0, Artificial Intelligence, and Communications Technology (IAICT). 2025. P. 508–513. doi: 10.1109/IAICT65714.2025.11101466
15. Fan L., Qi G. Frequency estimator of sinusoid based on interpolation of three DFT spectral lines // Signal Processing. 2018. V. 144. P. 52–60. doi: 10.1016/j.sigpro.2017.09.028

Authors

Duc Long Hoang — PhD, Lecturer, Le Quy Don Technical University, Hanoi, 10065, Vietnam, sc 57213158359, https://orcid.org/0000-0003-4975-9547, longhd@lqdtu.edu.vn

Anton A. Pyrkin — D.Sc., Full Professor, ITMO University, Saint Petersburg, 197101, Russian Federation, sc 26656070700, https://orcid.org/0000-0001-8806-4057, pyrkin@itmo.ru

Авторы

Хоанг Дык Лонг — PhD, преподаватель, Технический Университет Ле Куй Дона, Ханой, 10065, Вьетнам, sc 57213158359, https://orcid.org/0000-0003-4975-9547, longhd@lqdtu.edu.vn

Пыркин Антон Александрович — доктор технических наук, профессор, профессор, Университет ИТМО, Санкт-Петербург, 197101, Российская Федерация, sc 26656070700, https://orcid.org/0000-0001-8806-4057, pyrkin@itmo.ru

Статья поступила в редакцию 13.03.2026
Одобрена после рецензирования 17.06.2026
Принята к печати 20.07.2026

Received 13.03.2026
Approved after reviewing 17.06.2026
Accepted 20.07.2026